2023 45th Annual International Conference of the IEEE Engineering in Medicine & Biology Society (EMBC) | 979-8-3503-2447-1/23/$31.00 ©2023 IEEE | DOI: 10.1109/EMBC40787.2023.10340068

Camera Wavelength Selection for Multi-wavelength Pulse Transit Time based Blood Pressure Monitoring

Yukai Huang[1,2], Dongmin Huang[1], Jia Huang[4], Hongzhou Lu[4], Min He[2,3*], Wenjin Wang[1,*]

***Abstract*— Multi-wavelength pulse transmit time (MV-PTT) is a potential tool for remote blood pressure (BP) monitoring. It uses two wavelengths, typically green (G) and near-infrared (NIR), that have different skin penetration depths to measure the PTT between artery and arterioles of a single site of the skin for BP estimation. However, the impact of wavelength selection for MV-PTT based BP calibration is unknown. In this paper, we explore the combination of different wavelengths of camera photoplethysmography for BP measurement using a modified narrow-band camera centered at G-550/R-660/NIR-850 nm, especially focused on the comparison between G-R (full visible) and G-NIR (hybrid). The experiment was conducted on 17 adult participants in a dark chamber with their BP significantly changed by the protocol of ice water stimulation. The experimental results show that the MV-PTT obtained by G-NIR has a higher correlation with BP, and the fitted model has lower MAE in both the systolic pressure (5.78 mmHg) and diastolic pressure (6.67 mmHg) than others. It is confirmed that a hybrid wavelength of visible (G) and NIR is still essential for accurate BP calibration due to their difference in skin penetration depth that allows proper sensing of different skin layers for this measurement.**

***Index Terms*—Blood pressure, camera photoplethysmography, multi-wavelength, pulse transmit time.**

I. INTRODUCTION

Pulse transmit time (PTT) is a physiological parameter that records the transmission time of a pulse wave from the proximal to the distal end of the heart, which can be used for blood pressure (BP) monitoring [1]. In blood circulation, heart contraction-induced pulse waves are transmitted from deep to superficial vascular tissues [2]. In addition, since light photon penetrating through the skin is influenced by wavelength [3], different wavelengths of remote photoplethysmography (rPPG) carry information of pulse waves at different vascular tissues. Based on the above principles, earlier studies measured multi-wavelength pulse transmit time (MV-PTT) for BP monitoring [4], [5], where pulse waves from different vascular tissues can be extracted by two different wavelengths of rPPG and their phase delays can be calculated as MV-PTT. It is considered to be a potential method for cuffless and even contactless BP estimation.

Based on the measurement principle, the methods proposed for camera-based BP estimation can be divided into the following two categories [6]. The first category is the pulse waveform morphology-based method [7] that estimates BP by extracting the contour features of the pulse wave, which requires high-quality measurement of PPG signals and is susceptible to noise interference. The second category is the pulse transmit time based method [8]. In most prior arts, the rPPG signal is captured by multiple cameras focused at different body parts (e.g. face and palm) and PTT is calculated in between for BP estimation. The monitoring setup is more complicated in implementation and operation. Liu et al. [4] proposed a contact-based multi-wavelength PPG sensor that captures PTT from different skin layers for BP estimation. Slapnicar et al. [9] extended this concept to the contactless domain by using a narrow-band multi-wavelength camera to extract MV-PTT from different layers of skin tissues, where the near-infrared (NIR) and green (G) wavelengths were used. It has been shown that MV-PTT measures a single site of the skin, which does not involve different body parts and thus is easier to be implemented and used in practice. Also, it does not require the measurement of physical distance between two skin sites (e.g. body length) like multi-site PTT for BP calibration.

In this work, we investigate different wavelength sets to strengthen our understanding to this new measurement: full-visible and visible-NIR, where representative wavelengths of R, G and NIR are used for this investigation. Early studies showed that blue light cannot penetrate deep into arterioles nor arteries [9], thus blue wavelength was not in our consideration. We used rPPG signals from three independent channels of a modified narrow-band RGB camera for MV-PTT calculation: G (550 nm, with high pulsatility in the visible range), R (660 nm, used by ordinary RGB cameras and covered by common LED), and NIR (850 nm, the option suggested by [9] for MV-PTT). We combined these three channels two-by-two in pairs to calculate PTT, i.e. G-R (full visible), G-NIR (visible and NIR), and R-NIR (indicate the feasibility towards full-NIR). The experiment that investigates the above three wavelength combinations was conducted in a dark chamber, involving 17 volunteers with their BP significantly changed by the ice water stimulation, for obtaining a broader range of samples to validate the sensitivity and stability of BP estimation. We analyzed the correlation of three types of MV-PTTs with cuff-measured SBP and DBP, and fitted the PTT-BP model based on the

This work is supported by the National Key R&D Program of China (2022YFC2407800), General Program of National Natural Science Foundation of China (62271241), Guangdong Basic and Applied Basic Research Foundation (2023A1515012983), and Shenzhen Fundamental Research Program (JCYJ20220530112601003).

[1]Department of Biomedical Engineering, Southern University of Science and Technology, China.

[2]Hangzhou Institute of Medicine (HIM), Chinese Academy of Sciences, Hangzhou, Zhejiang 310022, China.

[3]Key Laboratory of Head Neck Cancer Translational Research of Zhejiang Province, Zhejiang Cancer Hospital.

[4]Intensive Care Unit, The Third People's Hospital of Shenzhen, China.

*Corresponding author: Min He (hemin607@163.com), Wenjin Wang (wangwj3@sustech.edu.cn)

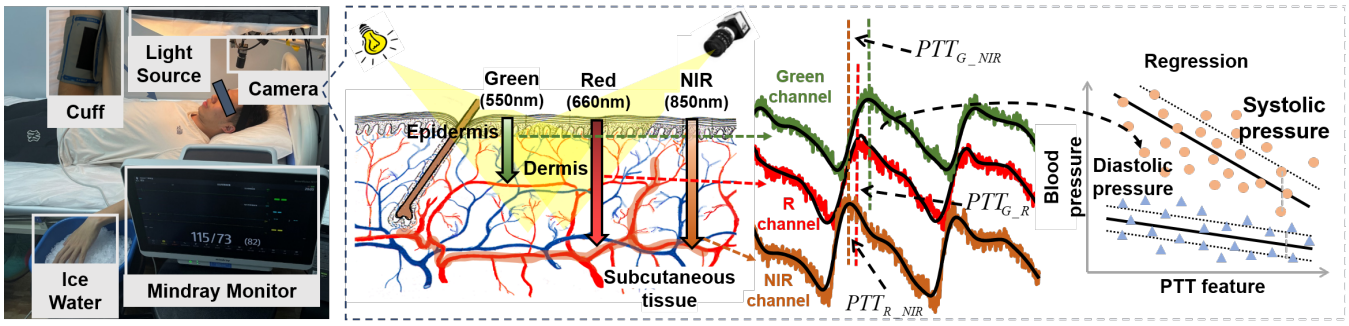

Fig. 1. Principle of investigated multi-wavelength PTT-BP measurement, including the experimental setup with the protocol of ice water stimulation.

least squares regression. Our preliminary results showed that the PTT calculated using rPPG in the G (550 nm) and NIR (850 nm) wavelengths has a higher correlation with BP and lower MAE in BP calibration than others.

II. METHODS

A. EXPERIMENTAL PROCEDURES

The trial collected real-time forehead videos and BP data from 17 healthy adult participants (3 females and 14 males, average age 24.2 ± 3.1 years). The experimental setup is shown in Fig. 1. The study was approved by the Institutional Review Board of Southern University of Science and Technology, and written informed consent were obtained from test participants. The detailed description of the experimental setting is as follows:

- Monitor (Mindray, BeneVision N17). It is used to collect the participant's BP as a reference, and the participant wears a cuff on the right arm during the measurement.
- Camera (IDS-UI3860C, 60 frames per second, 960×468 pixels). It is used to record the forehead video. The RGB camera is modified using a triple bandpass MidOpt TB550/660/850 filter by replacing its IR-block filter. In this way, the camera can capture light within the narrow bands of 550 ± 10 nm (green), 660 ± 10 nm (red), and 850 ± 22 nm (NIR) for MV-PTT measurement.
- Incandescent lamp (100 w bulb). It provides a continuous spectrum in 400-1700 nm that covers the visible and infrared parts, where the DC power (215 v, 150 w) supply is used to stabilize the illumination.
- Ice water. It is used to trigger a significant change in BP to verify the sensitivity of measurement. For healthy adult participants, SBP is increased by 10-20 mmHg, and DBP is increased by 5-15 mmHg, after about 1 min of ice water stimulation [10].

Each participant was required to participate two measurements with the same protocol in two separate weeks. The second experiment was performed one week after the first one. In each experiment, the participant was resting in the bed with a camera mounted $20-30$ cm above the forehead for stable recording. The Mindary monitor records 5 minutes of BP continuously where "continuous" means that one measurement starts right after the other. Each participant first underwent resting BP measurements for 3 BP measurement cycles, then began the ice water stimulation (constant grasping of the ice in the left hand) for 2 BP measurement cycles, and finally remained resting till the end of recording.

B. Data analysis

1) Data segmentation: The video recording and BP reference are synchronized during the data acquisition. Then the video is divided into segments with corresponding BP values according to the timestamps exported by the monitor.

2) rPPG signal extraction: The Maximum Between-Class Variance algorithm [11] is firstly used to select the skin area of the forehead videos as ROI (Region Of Interest). Then, the rPPG signals of G, R, and NIR channels are extracted from the ROI as G_{rPPG}, R_{rPPG}, and NIR_{rPPG}, respectively. Next, the following steps are performed on G_{rPPG}, R_{rPPG}, and NIR_{rPPG}:

- DC normalization. The DC component is normalized with zero-mean operation. The signals of three channels are shifted to the same origin, varying in the normalized range.
- Bandpass filtering. A 4-th order Butterworth filter with cut-off frequency $[0.5, 4.0]$ Hz is applied to remove the irrelevant frequency components.
- Newton resampling. Newton interpolation algorithm is applied to upsample rPPG signals from 60 Hz to 120 Hz. It is used to increase the temporal resolution for more accurate inter-beat interval (IBI) measurement between systolic peaks for PTT calculation.

3) PTT extraction: In blood circulation, blood pulse waves are transmitted from arteries to arterioles. And the rPPG signal at different wavelengths contains different pulsation information according to their penetration depths. Specifically, G (550 nm) penetrates into the dermis to obtain information related to arterioles, while R (660 nm) and NIR (850 nm) penetrate deeper into the subcutaneous tissue to access information about arteries. Therefore, the phase of the pulse waveforms of G, R and NIR channels have such relationships: G_{rPPG} lags behind R_{rPPG}, and R_{rPPG} lags behind NIR_{rPPG}. Such phase relationship allows the calculation of the time difference between the pulse wave transmission to different skin layers, further used for BP calibration. The rPPG signals obtained in G and NIR channels, G and R channels, and R and NIR channels, are used to calculate PTT features, denoted as PTT_{G_NIR}, PTT_{G_R}, and PTT_{R_NIR},

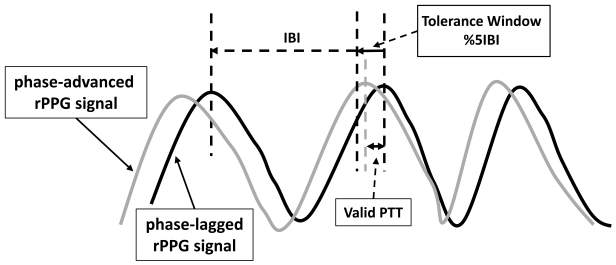

Fig. 2. The schematic diagram of PTT extraction. The tolerance window (0,5%IBI] is the adaptive PTT threshold, and the peak difference within the threshold is the valid PTT, outside is considered as the invalid PTT.

respectively. The schematic diagram of PTT extraction is shown in Fig. 2, with details specified below:

- Use the peak-detection algorithm to find systolic peaks of the phase-advanced rPPG signal and phase-lagged rPPG signal aligned with BP data, and calculate the IBI between systolic peaks per cardiac cycle.
- An outlier rejection range, $(0,5\% \cdot IBI]$ before the systolic peaks of the phase-lagged signal, is defined to reject the peaks detected outside this range. By physiological definition, the phase-lagged signal is always behind the phase-advanced signal due to the vascular structure, thus a lower threshold is determined, i.e. the lower limit of HR is 30 bpm and the upper limit of %5·IBI corresponds to the maximum of 100 ms. The definition of threshold is adaptive to the IBI and thus is subject-dependent.
- After calculating the PTT per beat, if the number of valid PTTs is more than $\frac{2}{3}$ of phase-lagged signal peaks, the average value of PTT is calculated per cycle from the segment, otherwise the segment is considered to be invalid.

C. Statistical analysis

To evaluate the performance of single-site MV-PTT for BP estimation, the experimental data from one week is applied to train the model, and the other week for testing. The mean absolute error (MAE) is used to evaluate the model performance. The model training methods are least squares based.

Since the PTT-based BP calibration is considered to be subject-dependent [12], generalized and individual BP calibration models are used to assess the performance of MV-PTT for BP calibration. The generalized model fits a model using data from all participants in one week experiment and using that model to predict BP for each participant in another week experiment. The individual model was designed for each participant to predict the BP, which was fitted using the data of one week from one participant and was tested using the data of other week from the same participant. The MAE of each participant is calculated and its mean value is calculated as the final MAE for the generalized model and individual model.

TABLE I

MEAN VALUES OF PCC BETWEEN BP AND THREE TYPES OF PTT FOR ALL PARTICIPANTS IN TWO WEEKS EXPERIMENT.

Setup	Week 1		Week 2	
	SBP	DBP	SBP	DBP
G&NIR	-0.77	-0.71	-0.82	-0.66
G&R	-0.46	-0.40	-0.54	-0.38
R&NIR	-0.38	0.11	-0.30	0.04

III. RESULTS AND DISCUSSION

A. Experimental settings

After removing the invalid data according to the definition in Fig. 2, 235 (week 1: 115, week 2: 120) $PTT_{G\_NIR} - BP$ data, 204 (week 1: 103, week 2: 101) $PTT_{G\_R} - BP$ data, and 107 (week 1: 57, week 2: 50) $PTT_{R\_NIR} - BP$ data were obtained for fitting and verification. Notably, 7 participants in the combination of R and NIR did not give enough valid PTT (i.e. R and NIR all reach arteries and the PTT in between is subtle), thus their data were discarded, so the number of $PTT_{R\_NIR} - BP$ data is less than others.

Fig. 3 shows the changes in three types of PTT before and after ice water stimulation in 2-weeks experiments. There is a significant decrease in PTT with the increase in BP after ice water stimulation, and such trend is reproducible in two separate weeks.

B. Correlation between BP and PTT

Based on [13], the correlation between BP and PTT can be represented by Pearson correlation coefficient (PCC), defined as high correlation (r < -0.7), moderate correlation (-0.7 < r < -0.4), and weak/no correlation (0 > r > -0.4).

Fig. 4 shows the PCC between three types of PTT and SBP/DBP for all participants in the 2-weeks experiments. The PTT_{G_NIR} has the highest correlation with SBP and DBP in both experiments, second by PTT_{G_R}, whereas PTT_{R_NIR} does not show a strong correlation with SBP/DBP.

Fig. 5 shows the PCC between three types of PTT and BP (SBP and DBP) for each participant. It shows that: (i) in week 1, the percentage of participants with high correlations of PTT and SBP are 82.4% (14/17, PTT_{G_NIR}), 17.6% (3/17, PTT_{G_R}) and 0% (PTT_{R_NIR}), and the percentage of participants with high correlations of PTT and DBP are 64.7% (11/17, PTT_{G_NIR}), 23.5% (4/17, PTT_{G_R}) and 0 (PTT_{R_NIR}); (ii) in week 2, the percentage of participants with high correlations of PTT and SBP are 82.4% (14/17, PTT_{G_NIR}), 35.3% (6/17, PTT_{G_R}) and 5.88% (1/17, PTT_{R_NIR}), and the percentage of participants with high correlations of PTT and DBP are 53.0% (9/17, PTT_{G_NIR}), 29.4% (5/17, PTT_{G_R}) and 0 (PTT_{R_NIR}).

Table I shows the averaged R-values of PCC between BP and PTT for all participants. It can be seen that PTT_{G_NIR} has the highest correlation with BP, followed by PTT_{G_R}, while PTT_{R_NIR} has almost no correlation with BP.

With the current setup, the performance ranking in terms of the correlation between PTT and SBP/DBP is: $PTT_{G\_NIR} >$

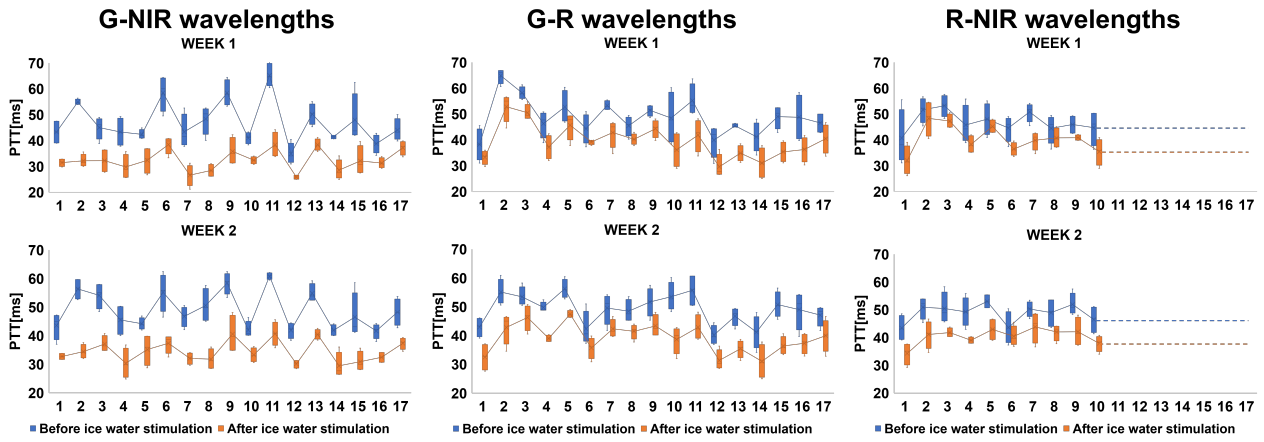

(a) (b) (c)

Fig. 3. Boxplots of PTT before and after ice water stimulation in week 1 and week 2. Since both R and NIR can reach artery, the PTT in between is subtle and even not observable. The participant without enough valid PTT is indicated by a dashed line.

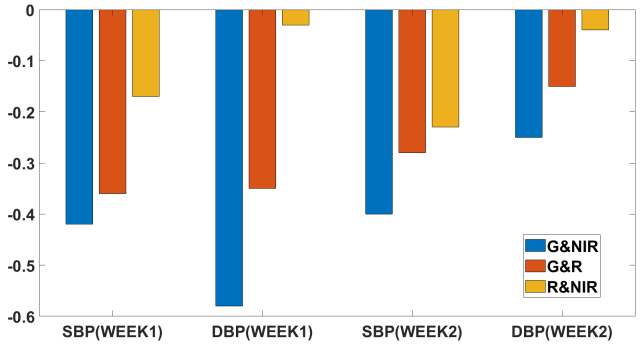

Fig. 4. PCC between BP and three types of PTT for all participants in the 2-weeks experiments. PTT and BP are negatively correlated.

$PTT_{G\_R} > PTT_{R\_NIR}$. PTT_{G_NIR} seems to be the most promising option of benchmark for BP calibration. PTT_{R_NIR} is not suitable for this measurement. Since R and NIR wavelengths can all reach the arterial situated in deeper skin layers, the time delay of PPG signals measured between R and NIR is obscure. The poor results of R-NIR wavelengths suggest that the full-NIR setup, where the penetration difference between two wavelengths is even smaller, is likely not possible for MV-PTT measurement.

C. PTT-based BP calibration

As seen above, the low correlation of PTT_{R_NIR} with BP is not feasible for BP calibration, so we only use PTT_{G_NIR} and PTT_{G_R} to calibrate BP and evaluate their performance in two types of modeling: generalized model and individual model.

In Table II, the first two rows show the MAE between the reference BP and camera-calibrated BP that uses the data from week 1 for calibration and week 2 for testing. The last two rows switch the calibration and testing data, i.e. week 2 used for calibration and week 1 used for testing.

Table II reports that the model fitted by PTT_{G_NIR} has a lower MAE than PTT_{G_R}. Individual models have lower MAE than generalized models, which is expected as the BP calibration has been reported to be subject-dependent [7], [12]. The individual variability is a major source of error for BP monitoring. For example, the pulse wave transmission velocity is influenced by the differences in vascular stiffness [14] and blood stickiness [15], resulting in different PTT in the time. And the skin tissue thickness affects the degree of light penetrating one site of the skin [3], leading to different PTT in the space. Those personalized factors influencing the calibration model should be further investigated.

TABLE II

MAE FOR CROSS-VALIDATION OF THE MODELS (GENERALIZED AND INDIVIDUAL) TRAINED AND TESTED ON DIFFERENT WEEKS.

Protocol	Setup [mmHg]	Generalized		Individual	
		SBP	DBP	SBP	DBP
Train on Week 1	G&NIR	5.97	6.82	5.78	6.67
Test on Week 2	G&R	6.57	7.52	6.55	7.16
Train on Week 2	G&NIR	6.64	7.32	6.19	7.24
Test on Week 1	G&R	7.65	8.32	6.90	8.02

In view of the above results, PTT_{G_NIR} derived by the combination of G and NIR channels is more promising for BP monitoring, as compared with G-R and R-NIR. PTT_{G_R} shows potential for BP measurement but its performance is clearly worse than the combination of G and NIR. We expect the limitations of the G-R setup to be twofold: (i) the distance between wavelengths of G and R is closer than that between G and NIR, thus the perceived skin layers are less distant; (ii) blood has low spectral absorption in the red wavelength, thus the quality of PPG signals measured from the R channel is generally worse than NIR. A full-visible setup (G and R) seems not favored for a solution aiming at highly-accurate BP monitoring. But as an ubiquitous non-clinical screening tool, a full-visible setup needs further investigation. For accurate BP measurement, we still recommend a hybrid setup with visible and NIR wavelengths for the MV-PTT measurement.

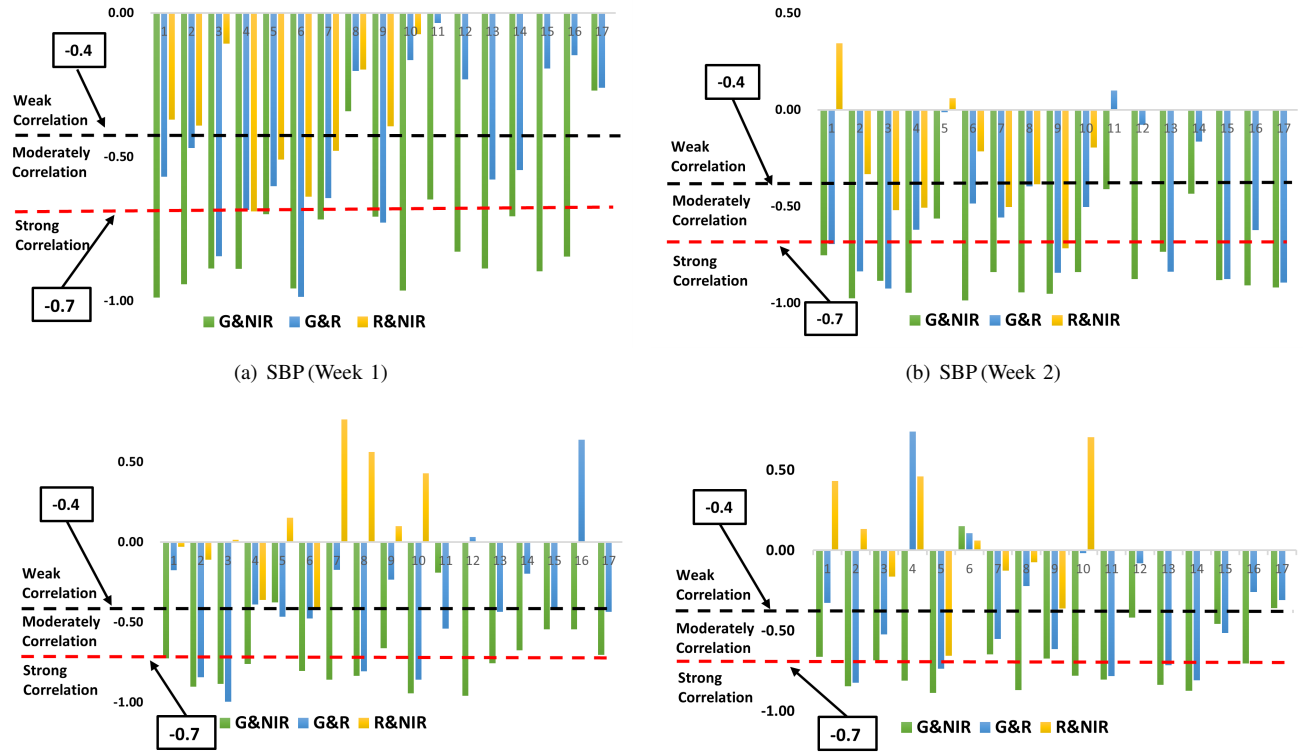

(a) SBP (Week 1)

(b) SBP (Week 2)

(c) DBP (Week 1)

(d) DBP (Week 2)

Fig. 5. Pearson correlation coefficient (R-value) between BP and PTT obtained for each participant in two separate weeks.

IV. CONCLUSIONS

In this work, we acquired multi-wavelength PTTs calculated from the combination of three different wavelengths of a narrow-band rPPG camera (G, R and NIR), and used MV-PTT for BP calibration. The reproducibility of multi-wavelength PTT was verified by cross-validation of experiments in two separate weeks. From the experimental results, MV-PTT has a high dependency on the selection of wavelength. The full-visible combination (G + R) is not accurate enough, and the R + NIR combination receives poor results, which indicates that full-NIR may not be feasible. The PTT calculated by visible + NIR is more stable and reliable, therefore, we consider that the combination of the visible and NIR wavelengths with a larger distance in skin penetration depth has better potential for accurate BP calibration. In the future, the studied approach will be evaluated in clinical trials involving ICU patients, where various intrinsic and extrinsic factors that may affect the BP calibration will be explored.

REFERENCES

[1] R. P. Smith *et al.*, "Pulse transit time: an appraisal of potential clinical applications," vol. 54, no. 5, pp. 452–457, 1999.

[2] R. E. Mehler, *How the circulatory system works*. John Wiley & Sons, 2014.

[3] L. Finlayson *et al.*, "Depth penetration of light into skin as a function of wavelength from 200 to 1000 nm," *Photochemistry and Photobiology*, vol. 98, no. 4, pp. 974–981, 2022.

[4] J. Liu *et al.*, "A preliminary study on multi-wavelength ppg based pulse transit time detection for cuffless blood pressure measurement," in *2016 38th Annual International Conference of the IEEE Engineering in Medicine and Biology Society (EMBC)*, 2016, pp. 615–618.

[5] J. Liu *et al.*, "Multi-wavelength photoplethysmography enabling continuous blood pressure measurement with compact wearable electronics," *IEEE Transactions on Biomedical Engineering*, vol. 66, no. 6, pp. 1514–1525, 2018.

[6] Y. Lu, C. Wang, and M. Q.-H. Meng, "Video-based contactless blood pressure estimation: A review," in *2020 IEEE International Conference on Real-time Computing and Robotics (RCAR)*, 2020, pp. 62–67.

[7] M. Rong and K. Li, "A blood pressure prediction method based on imaging photoplethysmography in combination with machine learning," *Biomedical Signal Processing and Control*, vol. 64, p. 102328, 2021.

[8] X. Fan *et al.*, "Robust blood pressure estimation using an rgb camera," *Journal of Ambient Intelligence and Humanized Computing*, vol. 11, no. 11, pp. 4329–4336, 2020.

[9] G. Slapničar, W. Wang, and M. Lučtrek, "Feasibility of remote pulse transit time estimation using narrow-band multi-wavelength camera photoplethysmography," in *2022 IEEE-EMBS International Conference on Biomedical and Health Informatics (BHI)*. IEEE, 2022, pp. 1–5.

[10] J. O. Godden *et al.*, "The changes in the intra-arterial pressure during immersion of the hand in ice-cold water," *Circulation*, vol. 12, no. 6, pp. 963–973, 1955.

[11] S. C. Satapathy *et al.*, "Multi-level image thresholding using otsu and chaotic bat algorithm," *Neural Computing and Applications*, vol. 29, pp. 1285–1307, 2018.

[12] D. Barvik *et al.*, "Noninvasive continuous blood pressure estimation from pulse transit time: A review of the calibration models," *IEEE Reviews in Biomedical Engineering*, vol. 15, pp. 138–151, 2022.

[13] P. Sedgwick, "Pearson's correlation coefficient," *Bmj*, vol. 345, p. e4483, 2012.

[14] Y.-X. Wang and R. M. Fitch, "Vascular stiffness: measurements, mechanisms and implications," *Current vascular pharmacology*, vol. 2, no. 4, pp. 379–384, 2004.

[15] D. Pitson *et al.*, "Value of beat-to-beat blood pressure changes, detected by pulse transit time, in the management of the obstructive sleep apnoea/hypopnoea syndrome," *European Respiratory Journal*, vol. 12, no. 3, pp. 685–692, 1998.